Random Walker Based Estimation and Spatial Analysis of Probabilistic fMRI Activation Maps

Bernard Ng[1], Rafeef Abugharbieh[1], Ghassan Hamarneh[2], Martin J. McKeown[3]

[1]Biomedical Signal and Image Computing Lab, Department of Electrical and Computer Engineering, The University of British Columbia.
[2]Medical Image Analysis Lab, Department of Computer Science, Simon Fraser University
[3]Department of Medicine (Neurology), Pacific Parkinson's Research Center
bernardn@ece.ubc.ca, hamarneh@cs.sfu.ca, rafeef@ece.ubc.ca,
mmckeown@interchange.ubc.ca

Abstract. Conventional univariate fMRI analysis typically examines each voxel in isolation despite the fact that voxel interactions may be another indication of brain activation. Here, we propose using a graph-theoretical algorithm called "Random Walker" (RW), to estimate probabilistic activation maps that encompass both activation effects and functional connectivity. The RW algorithm has the distinct advantage of providing a unique, globally-optimal closed-form solution for computing the posterior probabilities. To explore the implications of incorporating functional connectivity, we applied our previously proposed invariant spatial features to the RW-based probabilistic activation maps, which detected activation changes in multiple brain regions that conform well to prior neuroscience knowledge. In contrast, similar analysis on traditional activation statistics maps, which ignores functional connectivity, resulted in reduced detection, thus demonstrating benefits for integrating additional functional attributes into the activation detection procedures.

1 Introduction

Mass univariate analysis has by far been the most widely-used method for analyzing functional magnetic resonance imaging (fMRI) data. In this approach, each voxel is independently compared to an expected response to estimate the effects of activation. As a result, voxel interactions (i.e. functional connectivity), are ignored despite that each voxel is unlikely to be functioning in isolation. In fact, numerous past studies have shown the presence of task-related functional networks [1] and functional connectivity has actually been used as the basis for functional segmentation [2]. Thus, these findings suggest that functional connectivity may be another indication of brain activation and incorporating this additional information in estimating activation effects may help combat the inherently low signal-to-noise (SNR) in fMRI signals.

The idea of incorporating functional connectivity in activation detection has, in fact, been indirectly exploited in other past methods in the form of neighborhood information. For instance, Descombes et al. proposed modeling activation effect maps as Markov Random Fields (MRF) to encourage neighboring voxels to have similar

labels (e.g. active or non-active) [3]. Others proposed using Bayesian approaches to directly integrate neighborhood information into the activation effect estimates [4]-[6]. The underlying assumption is that neighboring voxels are likely to be functionally correlated, hence should exhibit similar activation levels. However, these methods typically model only correlations between immediate spatial neighbors due to computational complexity. Yet, considering that spatially-disconnected voxels may also jointly activate upon stimulus [1], modeling the interactions between spatially-disjointed voxels, in additional to immediate neighbors, may be beneficial.

Another limitation with standard mass univariate analysis is the need for spatial warping to generate a voxel correspondence across subjects. This correspondence is required for assessing the amount of inter-subject functional overlap to draw group inferences. However, due to anatomical and functional inter-subject variability, spatial warping tends to result in mis-registrations [7] and spatial distortions [8], which may render voxel-based group analysis inaccurate. To create a subject correspondence without spatial warping, a popular approach is to specify regions of interest (ROIs) and examine statistical properties of regional activation [9]. Under this ROI-based approach, group inferences are made by statistically comparing features extracted from the ROIs, such as mean activation statistics, across subjects. The underlying assumption is that the same anatomical ROIs across subjects pertain to similar brain functions. It is worth noting that this ROI-based approach is not directly comparable to conventional univariate group analysis, since subject correspondence is only established at a regional level, which precludes localization of common active voxels across subjects. Nevertheless, a more hypothesis-driven question of whether particular brain regions are activated is addressed, which is often the question of interest [7]. We have thus taken this region-based approach for the current study.

In this paper, we propose to estimate probabilistic activation maps using a graph-theoretic method called "Random Walker" (RW) that enables functional connectivity to be seamlessly integrated into the activation probability estimates. RW has the distinct advantage of providing an exact, unique, and globally-optimal closed-form solution for computing posterior probabilities [10]. Under the RW formation, voxels correspond to graph vertices with voxel interactions modeled as edge weights. Specifically, in the context of fMRI, activation effects are modeled through a likelihood term with functional connectivity encoded into a weighted graph Laplacian matrix for regularizing the likelihood. To infer group effects from the RW-based probabilistic activation maps under the ROI-based approach, characteristic features will first need to be defined and extracted from the probability maps. However, the optimal way for summarizing the regional activation probabilities is unclear. For instance, simply averaging the activation probabilities over an ROI and comparing these averages across subjects as done in standard ROI-based analyses [9] may be insufficient. Yet, if we consider the probabilistic activation maps as grayscale images, we can characterize the spatial distribution of regional activation, as reflected by the relative magnitude of the probability values, using invariant spatial features as we have previously proposed [11]. To explore the implications of incorporating functional connectivity, we contrast the sensitivity of the invariant spatial features derived from the RW-based probabilistic activation maps and the standard activation statistics maps (i.e. t-maps) in detecting group activation changes during a visuo-motor tracking experiment.

2 Materials

After obtaining informed consent, fMRI data were collected from 10 healthy subjects (3 men, 7 women, mean age 57.4 ± 14 years). Each subject used their left hand to squeeze a bulb with sufficient pressure such that a horizontal bar shown on a screen was kept within an undulating pathway. The pathway remained straight during baseline periods, which required a constant pressure to be applied. During the time of stimulus, the pathway became sinusoidal at a frequency of 0.25 Hz (slow), 0.5 Hz (medium) or 0.75 Hz (fast) presented in a pseudo-random order. Each session lasted 260 s, alternating between baseline and stimulus of 20 s duration.

Functional MRI was performed on a Philips Gyroscan Intera 3.0 T scanner (Philips, Best, Netherlands) equipped with a head-coil. T2*-weighted images with blood oxygen level dependent (BOLD) contrast were acquired using an echo-planar (EPI) sequence with an echo time of 3.7 ms, a repetition time of 1985 ms, a flip angle of 90°, an in plane resolution of 128×128 pixels, and a pixel size of 1.9×1.9 mm. Each volume consisted of 36 axial slices of 3 mm thickness with a 1 mm gap. A 3D T1-weighted image consisting of 170 axial slices was further acquired to facilitate anatomical localization of activation. Each subject's fMRI data was pre-processed using Brain Voyager's (Brain Innovation B.V.) trilinear interpolation for 3D motion correction and sinc interpolation for slice timing correction. Further motion correction was performed using motion corrected independent component analysis (MCICA) [12]. The voxel time courses were high-pass filtered to account for temporal drifts and temporally whitened using an autoregressive AR(1) model. No spatial warping or smoothing was performed. For testing our proposed method, we selected twelve motor-related ROIs, including the bilateral thalamus (THA), cerebellum (CER), primary motor cortex (M1), supplementary motor area (SMA), prefrontal cortex (PFC), and anterior cingulate cortex (ACC). Anatomical delineation of these ROI was performed by an expert based on anatomical landmarks and guided by a neurological atlas. The segmented ROIs were resliced at the fMRI resolution and used to extract the preprocessed voxel time courses within each ROI for subsequent analysis.

3 Methods

3.1 Probabilistic Activation Map Estimation Using Random Walker

Traditional ROI-based fMRI analysis typically draws group inference using features extracted from t-maps [9]. However, t-maps computed from conventional univariate approaches only model voxel-specific activation effects but not the functional interactions between voxels. Considering that such inter-voxel dependencies are also indications of brain activation, we propose estimating probabilistic activation maps that integrate activation effects and functional connectivity using RW [10], which provides an exact, unique closed-form solution for computing the posterior activation probabilities. Under the original RW formulation, voxels are treated as graph vertices with voxel interactions modeled as edge weights. The probability that a voxel belongs to a certain class label is then estimated by computing the probability that a random

walker starting at an unlabeled voxel will first reach each pre-labeled seed given the edge weights which bias the paths. This formulation, however, is not directly applicable to fMRI analysis since only voxel interactions are considered, which completely ignores intensity (i.e. activation effects in the context of fMRI). Also, pre-specifying a seed for every functional region within an anatomical ROI may not be possible. Therefore, we have adopted an extended RW formulation [10], where posterior activation probabilities are estimated by minimizing an energy functional that comprises an aspatial term (i.e. likelihood for modeling activation effects) and a spatial term (i.e. prior for modeling functional connectivity). This formulation is analogous to graph cuts (GC) approaches, where the aspatial and spatial terms in RW correspond to the data fidelity and label interaction terms in GC [10]. The key differences are that RW is non-iterative and minimizes the functional over the space of real numbers, instead of over discrete labels [10]. Since the relative activation level of the voxels defines the "texture" of the regional activation patterns, using probabilistic activation maps consisting of real numbers between [0,1], as estimated using RW, enables such textural information to be modeled in our spatial analysis.

Simulating all possible paths that a random walker may take is computationally infeasible. Fortunately, it has been shown [10] that the posterior probabilities p^s of the voxels within an ROI being assigned a label s given data can be estimated by solving:

$$\left(L + \sum_{r=1}^{N_c} \Lambda^r \right) p^s = \lambda^s , \qquad (\mathbf{1})$$

where λ^s is a column vector containing the likelihood of the voxels being assigned label s as estimated based on the t-statistics, Λ^s is a matrix with λ^s along its diagonal, and N_c is the number of class labels. Due to the presently unclear interpretation of negative t-statistics [13], we restrict our analysis to only positive t-statistics. Hence, voxels are designated as either active or non-active (i.e. 'de-active' is not considered). L is a weighted graph Laplacian matrix. To estimate the likelihood λ^s, we first compute the t-statistics using a general linear model (GLM) with boxcar functions convolved with the hemodynamic response as regressors. Two mixtures of distributions are compared for modeling the t-statistics, namely a mixture of two Gaussians (GMM) and a mixture of Gamma and Gaussian (GGM) with the Gamma distribution used to model the activated voxels [6]. Specifying the parameter values of these distributions a priori, however, can be very challenging. Therefore, we employ the expectation maximization (EM) algorithm to learn the GMM parameters [14]. As for estimating the GGM parameters, since no widely-accepted formulation is present, an iterative method we refer to as the simplified-EM algorithm is employed:

Initialization: Label the voxels as active or non-active based on the GMM posterior probability estimates. Assuming the active voxels have t-statistics, $t_i \sim Gamma(\alpha, \beta)$, estimate α and β. Equations for estimating α and β can be found in e.g. [15]. For the non-active voxels, we assume $t_i \sim N(\mu, \Sigma)$ and estimate μ and Σ as the sample mean and covariance.

E-step: Compute $Gamma(t_i; \alpha, \beta)$ and $N(t_i; \mu, \Sigma)$ for all voxels and re-label the voxels based on maximum likelihood.

M-step: Based on the re-assignment, update α, β, μ, and Σ.

Convergence: Repeat the *E* and *M* steps until no re-assignment occur. The resulting α, β, μ, and Σ are used to estimate the likelihood λ^s.

The simplified-EM algorithm is similar to EM except a hard assignment, instead of posterior probabilities, is used in the E-step. Since RW only requires the likelihood λ^s as input, this algorithm is sufficient for our current application. We note that to decouple amplitude effects from spatial changes, as further discussed in Section 3.2, we have fitted a separate mixture model for each experimental condition. Specifically, if the t-statistics are generally larger during the fast condition for example, we will like to remove this overall amplitude change from our spatial analysis so that any detected changes in our spatial features will not be due to amplitude effects. This can be achieved by fitting a separate mixture for each condition so that the centers of the mixtures can adapt to the amplitude of the t-statistics during the different conditions.

To integrate functional connectivity into p^s, we define L as follows:

$$L_{ij} = \begin{cases} -w_{ij} = corr(I_i(t), I_j(t)), & i \neq j \\ d_i = \sum_{j \in N_i} w_{ij}, & i = j \end{cases}, \quad (2)$$

where $I_k(t)$ is the intensity time course of voxel k and N_i is the neighborhood of voxel i. In this work, we model the ROIs as fully-connected graphs to incorporate both correlations between immediate neighbors and spatially-disconnected voxels. However, some voxel correlations may have arisen due to blood flow or residual movement artifacts that remained after preprocessing. Therefore, we set all w_{ij} below a threshold to 0, where the threshold is determined by examining the distribution of correlation values between signals generated from AR(1) processes: $\varepsilon_k(t+1) = a\varepsilon_k(t) + \sigma_k(t)$, $\sigma_k(t)$ being a white Gaussian noise process and a is set to 0.3 as typically observed in the residuals of real fMRI data. A threshold of 0.7 is applied to remove 99.7% of the probability density from the null distribution. Note that we have used correlations instead of differences in t-statistics in (2) to account for cases where voxels may have similar t-statistics but are only mildly correlated. For example, in a block design experiment as employed in this study, if voxel i responds during the beginning of a block, whereas voxel j responds near the end of the block, these voxels will display similar t-statistics yet will not be highly correlated.

3.2 Group Spatial Analysis

In standard ROI-based analysis, amplitude-based features, such as mean t-statistics, are often used to summarize the ROI response. Group inferences are then drawn by statistically comparing the ROI features across subjects. However, simply averaging the t-statistics neglects potential spatial changes. Therefore, we proposed previously to use invariant spatial features to characterize the ROI activation patterns [11]. Using these spatial features enables a compact or focused pattern to be distinguished from a diffused activation pattern for example. Also, the invariance properties of these features facilitate comparisons of activation patterns in the subjects' native space [11]. In this work, we examine activation changes using one such feature, J_1, that is specific for measuring the spatial extent of activation relative to the activation centroid:

$$J_1 = \mu_{200} + \mu_{020} + \mu_{002}, \quad (3)$$

$$\mu_{pgq} = \iiint (x_s - \bar{x}_s)^p (y_s - \bar{y}_s)^q (z_s - \bar{z}_s)^r \rho(x_s, y_s, z_s) dx_s dy_s dz_s, \quad (4)$$

where $n = p+q+r$ is the order of the centralized 3D moment, μ_{pqr}, $\rho(x_s,y_s,z_s)$ is the probability of a voxel located at (x_s,y_s,z_s) being active as estimated using RW, $(\bar{x}_s, \bar{y}_s, \bar{z}_s)$ are the centroid coordinates of $\rho(x_s,y_s,z_s)$, and (x_s,y_s,z_s) are the (x,y,z) coordinates of the voxels scaled to account for ROI size differences:

$$x_s = x/s,\ y_s = y/s,\ z_s = z/s, \quad s = \sqrt{\sum_{i \in ROI}((x_i - \bar{x})^2 + (y_i - \bar{y})^2 + (z_i - \bar{z})^2)}\ , \tag{5}$$

where $(\bar{x}, \bar{y}, \bar{z})$ is the anatomical centroid of a given ROI. In [11], we normalized the t-statistics by the maximum to decouple amplitude effects from spatial changes, which enables a diffused activation pattern with mild activation effects to be distinguished from a focused pattern with high activation amplitude. Now, with $\rho(x_s,y_s,z_s)$ being probability maps bounded between [0,1], this step is no longer required. Also in [11], we obtained scale invariance by $\mu_{pqr} \big/ \mu_{000}^{(p+q+r)/3+1}$, which may pool residual amplitude effects after t-statistics normalization into the spatial analysis. Here, we instead employ (5), which does not involve $\rho(x_s,y_s,z_s)$, to account for size differences.

For comparisons, we compute J_1 with $\rho(x_s,y_s,z_s)$ being t-statistics normalized by the maximum as well as using a sigmoid function:

$$\rho_{norm}(x_s, y_s, z_s) = 1/(1 + \exp(-\sigma \cdot \rho(x_s, y_s, z_s)/\rho_{\max}))\ , \tag{6}$$

where ρ_{max} is the 99th percentile of $\rho(x_s,y_s,z_s)$ and σ is chosen such that outlier voxels with $\rho(x_s,y_s,z_s) > \rho_{max}$ are saturated to 1. σ is set to 5 in this paper.

4 Results and Discussion

Probabilistic activation maps generated using RW are shown in Fig. 1. Compared to standard t-maps, incorporating functional connectivity resulted in sharper activation maps with voxels displaying moderate activation effects and low (high) functional connectivity suppressed (reinforced). Increasing frequency led to a focusing of the activation pattern in the left thalamus as evident by comparing Fig. 1(a) and (b) but less apparent in (c) and (d). We note that observing fewer voxels recruited at higher frequency may seem counter-intuitive, but this finding can be explained by the increase in t-statistics of the recruited voxels during the fast condition (albeit not significant compared to the slow condition, Fig. 2), thus suggesting that certain brain regions adapt to higher frequencies by increasing activation at task-specific locations.

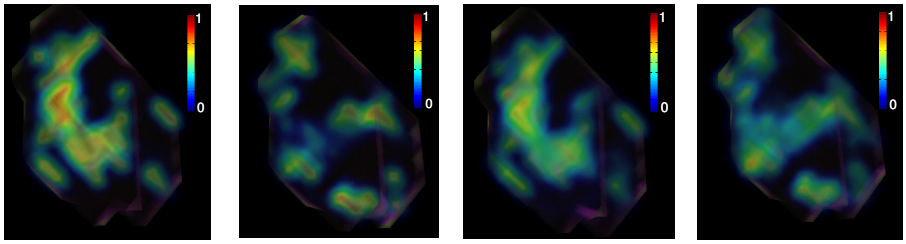

(a) RW, slow (b) RW, fast (c) t-map, slow (d) t-map, fast

Fig. 1. Activation maps of left thalamus of an exemplar subject. RW probabilistic activation maps appear sharper than the t-maps (normalized using (6)). Increasing frequency resulted in a focusing of the activation patterns as evident in (a) and (b) but less apparent in (c) and (d).

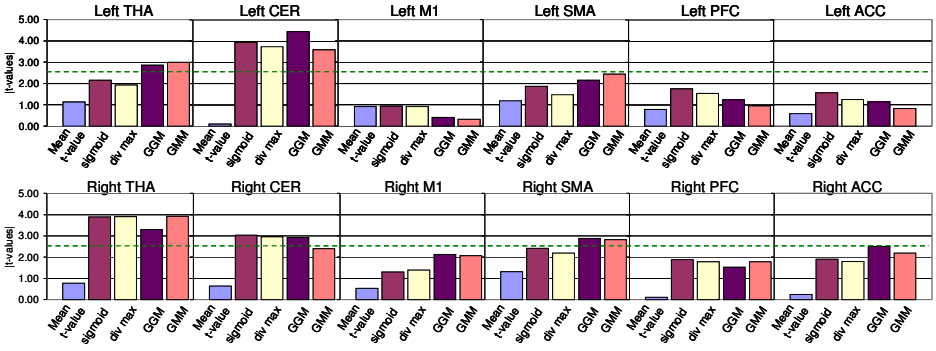

Fig. 2. Real fMRI data results. t-values obtained by applying a paired t-test to J_1 of the slow and fast conditions are displayed. Significance is declared at a t-threshold of 2.64 as indicated by the green dashed line. From left to right, the five bars pertain to using mean t-statistics, J_1 with t-maps normalized using a sigmoid function, dividing by the maximum, *proposed probabilistic activation maps* with t-statistics modeled using GGM and GMM. J_1 based on t-maps detected the right thalamus and bilateral cerebellar hemispheres, whereas no significance was found with mean t-statistics. Using GGM detected the left thalamus and right SMA in additional to ROIs found with t-maps, thus suggesting potential benefits for incorporating functional connectivity.

Quantitative results comparing J_1 derived from RW probabilistic activation maps and t-maps are summarized in Fig. 2. Only results contrasting J_1 of the slow and fast conditions using a paired t-test are presented due to space limitation. Significance is declared at a t-threshold of 2.64, corresponding to a p-value of 0.05 with false discovery rate (FDR) correction. Traditional mean t-statistics were also examined.

Using mean t-statistics, no significant task-related activation changes were detected in any of the ROIs. In contrast, applying J_1 to normalized t-maps (i.e. divided by the maximum as proposed in [11]) detected the right thalamus and the bilateral cerebellar hemispheres, thus again demonstrating the importance of incorporating spatial information. Tracking tasks such as the one employed in this work is known to activate the cerebello-thalamo-cortical motor pathway [16]. Thus, detecting the right thalamus and the bilateral cerebellar hemispheres conforms to prior neuroscience knowledge. Normalizing the t-maps using a sigmoid function detected the same ROIs but with higher discriminability in the left cerebellum. This increase is likely due to outlying t-statistics being saturated to 1 by the sigmoid function. Applying J_1 to the proposed probabilistic activation maps with voxel t-statistics modeled using a GGM detected the left thalamus and the right SMA, in addition to ROIs found with t-maps. Examining Fig. 1, incorporating functional connectivity resulted in more discriminant activation patterns, which may explain the additional ROI detections. These results are consistent with past findings, since the left thalamus and the right SMA are also part of the cerebello-thalamo-cortical motor pathway [16]. Modeling the voxel t-statistics using GMM detected significant activation changes in the same ROIs as those found with GGM, except for a loss of detection in the right cerebellum, which fell just below the t-threshold. This suggests that using a Gamma distribution is more suitable for modeling the t-statistics of the active voxels than using a Gaussian distribution, as was previously observed [6].

5 Conclusions

In this paper, we propose estimating fMRI probabilistic activation maps using RW, which guarantees global optimality of the posterior activation probability estimates. The flexibility of the RW formulation enables functional connectivity information to be easily integrated into the probabilistic activation maps. Applying invariant spatial features to the RW-based probabilistic activation maps detected significant activation changes in multiple ROIs known to be invoked in tracking tasks, whereas reduced sensitivity was observed when similar spatial analysis was performed on traditional t-maps. Our results thus suggest that incorporating additional functional attributes in the activation estimation procedures may be a promising direction to explore.

References

1. Rogers, B.P., Morgan, V.L., Newton, A.T., Gore, J.C.: Assessing Functional Connectivity in the Human Brain by fMRI. Magn. Reson. Imaging. 25, 1347-1357 (2007)
2. Lohmann, G., Bohn, S.: Using Replicator Dynamics for Analyzing fMRI Data of the Human Brain. Trans. Med. Imaging. 21, 485--492 (2002)
3. Descombes, X., Kruggel, F., von Cramon, D.Y.: Spatio-Temporal fMRI Analysis Using Markov Random Fields. Trans. Med. Imaging. 17, 1028--1039 (1998)
4. Penny, W.D., Trujillo-Barreto, N.J., Friston, K.J.: Bayesian fMRI Time Series Analysis with Spatial Priors. NeuroImage. 24, 350--362 (2005)
5. Harrison, L.M., Penny, W.D., Asburner, J., Trujillo-Barreto, N.J., Friston, K.J.: Diffusion-based Spatial Priors for Imaging. NeuroImage. 38, 677--695 (2007)
6. Woolrich, M.W., et al.: Mixture Models with Adaptive Spatial Regularization for Segmentation with an Application to fMRI Data. Trans. Med. Imaging. 24(1), 1--11 (2005)
7. Thirion, B., et al.: Dealing with the Shortcomings of Spatial Normalization: Multi-subject Parcellation of fMRI Datasets. Hum. Brain Mapp. 27, 678--693 (2006)
8. Ng, B., Abugharbieh, R., McKeown, M.J.: Adverse Effects of Template-based Warping on Spatial fMRI Analysis. In: Proc. SPIE. 7262, 72621Y (2009)
9. Constable, R.T., et al.: Quantifying and Comparing Region-of-Interest Activation Patterns in Functional Brain MR Imaging: Methodology Considerations. Magn. Reson. Imaging. 16(3) 289--300 (1998)
10. Grady, L.: Multilabel Random Walker Image Segmentation Using Prior Models. In: Proc. IEEE Comp. Soc. Conf. Comp. Vision Pattern Recog. 1, 763--770 (2005)
11. Ng, B., Abugharbieh, R., Huang, X. McKeown, M.J.: Spatial Characterization of fMRI Activation Maps Using Invariant 3-D Moment Descriptors. Trans. Med. Imaging. 28(2), 261-268 (2009)
12. Liao, R., Krolik, J.L., McKeown, M.J.: An Information-theoretic Criterion for Intrasubject Alignment of fMRI Time Series: Motion Corrected Independent Component Analysis. Trans. Med. Imaging. 24(1), 29--44 (2005)
13. Harel, N., et al.: Origin of Negative Blood Oxygenation Level-Dependent fMRI Signals. J. Cereb. Blood Flow Metab. 22(8) 908--917 (2002)
14. Bishop, C.M.: Pattern Recognition and Machine Learning. Springer Science+Business Media, LLC, New York (2007)
15. Coit, D.W., Jin, T.: Gamma Distribution Parameter Estimation for Field Reliability Data with Missing Failure Times. IIE Trans. 32, 1161--1166 (2000)
16. Miall, R.C., Reckess, G.Z., Imamizu, H.: The Cerebellum Coordinates Eye and Hand Tracking Movements. Nat. Neurosic. 4, 638--664 (2001)